

Versatile and Switchable Responsive Properties of a Lanthanide-Viologen Metal–Organic Framework

 HPSTAR
698-2019

Teng Gong, Qi Sui, Peng Li, Xian-Fu Meng, Li-Jiao Zhou, Jinqian Chen, Jianhua Xu, Lin Wang, and En-Qing Gao*

Metal–organic frameworks (MOFs) provide intriguing platforms for the design of responsive materials. It is challenging to mobilize as many components as possible of a MOF to collaboratively accomplish multiple responsive properties. Here, reversible photochromism, piezochromism, hydrochromism, ionochromism, and luminescence modulation of an ionic Eu(III) MOF is reported furnished by cationic electron-deficient viologen units and exchangeable guest anions. Mechanistically, the extraordinarily versatile responsive properties are owed to electron transfer (ET), charge transfer (CT), and energy transfer, involving viologen as electron acceptor, anion as electron donor, luminescing Eu(III) as energy donor, and anion-viologen CT complex or ET-generated radical as energy acceptor (luminescence quencher). Moreover, guest anions and waters provide flexible handles to control the ET-based responsive properties. Water release/reuptake or exchange with organic solvents can switch on/off the response to light, while reversible anion exchange can disable or awaken the responses to pressure, light, and water release/reuptake. The impacts of water and anions on ET are justified by the high polarity and hydrogen-bonding capability of water, the different electron donor strength of anions, and the strong I⁻-viologen CT interactions. The rich responsive behaviors have great implications for applications such as pressure sensors, iodide detection, and chemical logic gates.

1. Introduction

Stimuli-responsive materials that exhibit changes in light absorption or emission properties upon exposure to external stimuli (such as light, pressure, electricity, and chemical/biological molecules) are the basis of many applications such as information technology, sensors, and medical diagnosis.^[1] Metal–organic frameworks (MOFs) are emerging as intriguing platforms for the design of responsive materials.^[2] The hybrid crystalline networks can in principle be imparted with various responsive properties through functionalizing the metal-based joints, the organic structs, and the pore space or utilizing the cooperative effects between these components.^[2] It would be interesting if all of the components could be mobilized to collaboratively implement multiple responsive properties.

The electron-poor viologen unit (V²⁺, 4,4'-bipyridinium) has strong proneness to form charge-transfer (CT) complexes, to undergo electron transfer (ET) and to induce energy transfer (EnT),^[3] so it has attracted much attention as a versatile

responsive building unit for photo/electrochromic materials,^[4] chemical sensors/switches,^[5] host–guest assemblies, and molecular machines.^[6] The ET activity also underlies the applications of viologen compounds as herbicides in agriculture and as electron relays in photocatalytic systems.^[7] Encouraged by the fascinating properties of the viologen unit, many coordination polymers with viologen-derived ligands (especially those with carboxylate groups) have been synthesized in recent years.^[8] The metal–organic hybridization not only modulates the viologen-based chromogenic properties but also can impart new responsive properties, such as stimulus-modulated luminescent,^[9] magnetic,^[10] nonlinear optical,^[11] conductive,^[12] and piezoelectric properties.^[8,13] However, most of these coordination polymers are nonporous or easily undergo framework collapse. Only a few viologen-based MOFs with permanent porosity have been reported, which exhibit interesting adsorption properties for ammonia or other electron donor molecules.^[5,9,14] We recently obtained a unique lanthanide-viologen ionic MOF (LVMOF-1) exhibiting permanent open

Dr. T. Gong, Dr. Q. Sui, P. Li, X.-F. Meng, L.-J. Zhou, Prof. E.-Q. Gao
Shanghai Key Laboratory of Green Chemistry and Chemical Processes
School of Chemistry and Molecular Engineering
East China Normal University
Shanghai 200062, China
E-mail: eqgao@chem.ecnu.edu.cn

Prof. J. Chen, Prof. J. Xu
State Key Laboratory of Precision Spectroscopy
East China Normal University
Shanghai 200062, China

Prof. L. Wang
Center for High Pressure Science and Technology
Advanced Research
Shanghai 201203, China

 The ORCID identification number(s) for the author(s) of this article can be found under <https://doi.org/10.1002/sml.201803468>.

DOI: 10.1002/sml.201803468

channels and excellent chemical tolerance in various media including water.^[15] The viologen moieties furnishing the channels are ideally spaced (≈ 7 Å) for sandwiching electron-rich benzene derivatives through CT interaction, representing an infinite array of Stoddart's "blue box" (a rectangular cyclophane formed by two p-xylylene groups spacing two viologen groups^[16]). We demonstrated that the MOF undergoes sensitive color and luminescence changes in response to phenols and anilines, affording fast and ultratrace sensing in aqueous media.^[15] Considering the versatile responsive capabilities of viologen, we presume that the MOF is potentially responsive to various stimuli besides electron-rich aromatic molecules, such as light, heat, and pressure. Furthermore, we expect that the stable porous and cationic framework can allow reversible solvent evacuation/exchange and anion exchange without structural collapse, so the solvent and the anion may provide new dimensions to induce or modulate responsive properties. With these in mind, here we report the extraordinarily versatile responsive properties of **LVMOF-1**. As illustrated in **Figure 1**, all of the components (the viologen moiety, the Eu(III) center, the anion, and also the guest solvent) in the MOF are mobilized to be directly or indirectly involved in ET, CT, and EnT. Because of radical formation through ET, the MOF with Cl^-/Br^- undergoes reversible color changes in response to water release and reuptake (hydrochromism), to photoirradiation after evacuation or in organic solvents (photochromism), and to high pressure (piezochromism). Anion exchange with superhalogen ions disables the above ET-based responses for lack of electron donors, while iodide suppresses the ET-based responses and induces ionochromism owing to strong iodide-viologen CT complexation, which is confirmed by single-crystal structure analysis. Quenching effects on Eu^{3+} luminescence are concomitant with the ET and CT based chromogenic processes, owing to EnT from Eu^{3+} to radicals or CT complexes. The versatile responsive properties of the MOF impel us to explore its use in logic gates and anion sensors.

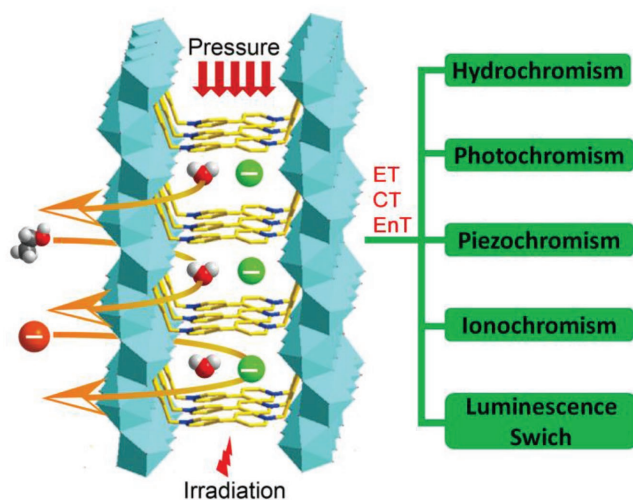


Figure 1. Schematic illustration of the multiple-response properties of **LVMOF-1**.

2. Results and Discussion

2.1. Multistimuli Responsive Properties Associated with Radical Formation

The responsive properties were first investigated using the as-synthesized MOF,^[15] which contains chloride as counterion (**LVMOF-1-Cl**). It changes color in response to a variety of stimuli (**Figure 2a**). First, it shows reversible color change upon water release and reuptake. It turns from pale-yellow to green upon heating at 100–150 °C, which corresponds to the release of the guest water in the channel according to thermogravimetric analysis. Powder X-ray diffraction (PXRD) indicated that the framework remains unchanged after evacuation at 150 °C (**Figure S1**, Supporting Information). As shown in **Figure 2b**, the evacuated green state displays broad visible-light absorption in the 500–800 nm range (λ_{max} , 620 nm), which is absent in the pristine state. The green state shows an ESR (electron spin resonance) signal at $g = 2.0038$ (**Figure 2c**). The results indicate the formation of radicals through ET to the viologen chromophore.^[17] The green state is also accessible by slow room-temperature dehydration in a desiccator containing concentrated sulfuric acid, either in natural light or in the dark, so the radical formation does not need light or heating. Heating promotes the process just by accelerating evacuation of the channels. On the other hand, the radical-containing green state is stable in dry air for at least one year but rapidly recovers to yellow in moist atmosphere, either air or nitrogen, suggesting that the reverse process does not involve radical quenching by molecular oxygen. Therefore water release or reuptake is the sole effective stimulus that triggers forward or back ET, which generates or annihilates radicals, respectively. The phenomenon that a substance changes color on exposure to water has been termed "hydrochromism."^[18] The switching between the green and yellow states of **LVMOF-1-Cl** is induced by water release/reuptake, representing a type of reversible hydrochromism involving the ET-active viologen chromophore.^[1b,19] The ET-based organic hydrochromic behaviors phenomenologically resemble but mechanistically differ from the properties of many transition-metal compounds (for example, CoCl_2), where the change in ligand field is responsible for the color change concomitant with (de)hydration.

LVMOF-1-Cl shows dehydration- and solvent-assisted photochromism. The pristine pale-yellow state did not change color upon prolonged irradiation under a 300 W Xe lamp, but the water-evacuated green state quickly turns blue under the Xe lamp. UV-vis and ESR spectra (**Figure 2b,c**) suggest that the radical concentration is increased through photoinduced ET (PET). In addition, the pristine yellow crystals immersed in various organic solvents (alcohols, acetonitrile, *N,N*-dimethylformamide, dimethyl sulfoxide, ether, acetone, tetrahydrofuran, hexane, or toluene) turn blue or blue violet immediately upon Xe-light irradiation (**Figure 2a** and **Figure S2**, Supporting Information). By contrast, the solid in water is silent to Xe-light irradiation. The photogenerated states, either from the dehydrated sample or from solvent-immersed samples, are stable in dry nitrogen but quickly turn green in dry air, suggesting partial radical quenching by molecular oxygen. They return directly to the pristine yellow state on exposure to moist atmosphere

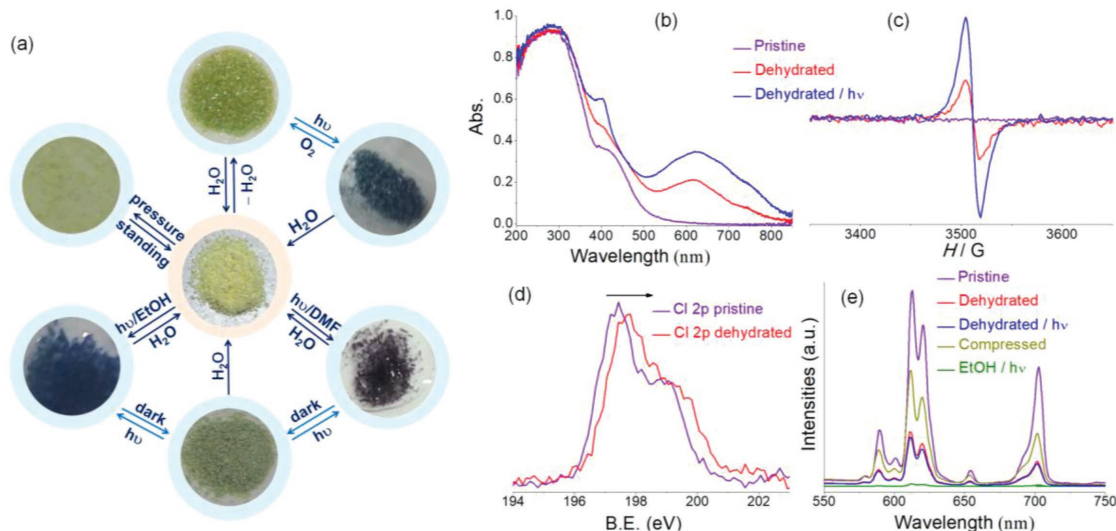


Figure 2. Multistimuli-responsive properties of LVMOF-1-Cl associated with radical formation. a) Photographic images showing the reversible color changes of polycrystalline samples in response to various physical and chemical stimuli. b) UV-vis and c) ESR spectra for the pristine state and the evacuated states before and after Xe-light irradiation. d) XPS spectra before and after evacuation. e) Comparison of the photoluminescence spectra (excited at 394 nm) before and after subjection to various stimuli.

(either air or nitrogen). This implies that water serves to induce back ET to completely annihilate the radicals.

LVMOF-1-Cl is also piezochromic. It turns green after compression using a hydraulic press (Figure 2a). UV-vis and ESR spectra also indicate the formation of radicals (Figure S3, Supporting Information), which proceeds through piezoinduced ET (PzET). High-pressure in situ UV-vis spectroscopy of a single crystal was performed using the diamond anvil cell (DAC) technique, which provides isotropic hydrostatic pressure in contrast with the uniaxial pressure of a hydraulic press. As shown in Figure 3a and Figure S4a in the Supporting Information, broad visible-light absorption at 550–750 nm appears at ≈ 2 GPa and the maximum absorbance increases quasi-linearly with pressure, indicating the onset of radical formation and the increase of radical content. The band maximum is redshifted with pressure. After complete decompression, the radical absorption is retained but with decreased intensity (Figure S4b, Supporting Information). The phenomena suggest that back ET occurs but does not keep pace with the decompression process, leaving a certain portion of radicals after complete removal of

pressure.^[19a,20] However, if kept at ambient pressure for hours, the green sample, either obtained from hydraulic presses or from DACs, completely returns to the original yellow color. The reverse process is independent of the atmosphere, indicating that the piezoinduced state is metastable and decays through spontaneous back ET (that is, no external stimulus is needed). Notably, viologen-based piezochromism through PzET is a very recent discovery,^[10b,19a,b,20] and LVMOF-1 represents the first porous MOF exhibiting such kind of piezochromism.

The stability of the material against stimuli and the reversibility of the chromogenic phenomena are very important for many applications such as switches and sensors. To our satisfaction, the crystalline framework is retained after exposure to all abovementioned stimuli (Figure S5, Supporting Information), and all of the abovementioned chromogenic processes are reversible.

All of the above chromogenic phenomena involve the reduction of V^{2+} to V^{+} through ET. Potential electron sources in the structure are the carboxylate group, the μ -hydroxo group, the water molecules (as ligand or guest), and the chloride anion. The ET pathways in viologen-based crystals are short

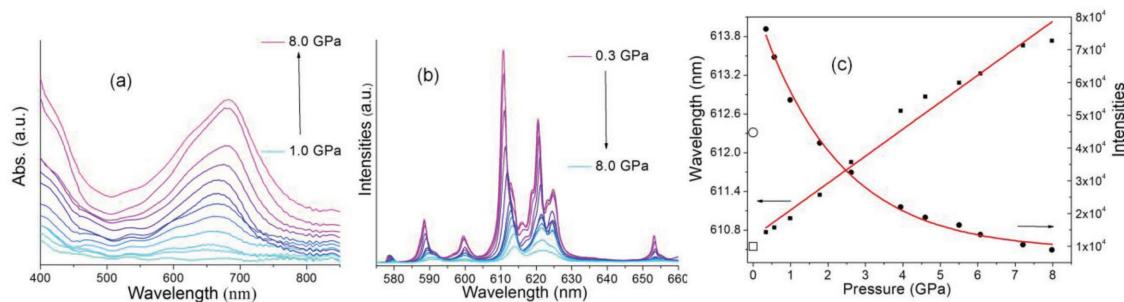


Figure 3. In situ UV-vis a) absorption and b) emission (excited at 532 nm) spectra of LVMOF-1 upon compression using DACs. c) Pressure dependence of the maximum wavelength and intensity of the Eu(III) $^5D_0 \rightarrow ^7F_2$ emission during compression (solid symbol) and after complete decompression (open symbol). The red lines represent the fitting curves.

donor-viologen contacts.^[4b,10a,21] In the rod-crosspiece structure of **LVMOF-1-Cl**, the hydroxo, carboxylate, and water ligands that constitute the rod-like building blocks are kept far apart from the viologen chromophore in the crosspiece, so these coordinated groups can be excluded from electron donors. The fact that the pristine **LVMOF-1** is not photochromic but release of guest water leads to radical formation and photochromism suggests that the guest water molecules are not donors but a kind of detrimental factor in ET. This is consistent with previous studies on MV^{2+} (dimethyl viologen) in aqueous solutions, which concluded that MV^{2+} cannot be photoreduced by water because of the high ionization potential (IP) of water (12.62 eV).^[22]

Thus, the only remaining donor is Cl^- . We reexamined the single-crystal structure for possible ET pathways between Cl and viologen. As shown in **Figure 4**, Cl^- is weakly hydrogen-bonded to viologen with $H_V \cdots Cl = 2.72\text{--}2.95$ Å. Solid evidence comes from X-ray photoelectron spectroscopy (XPS, **Figure 2d**). The Cl $2p_{3/2}$ and $2p_{1/2}$ peaks (197.6 and 199.1 eV) for the evacuated green state show appreciable hypsochromic shifts compared with the pristine state (197.3 and 198.9 eV), clearly evincing electron loss from Cl^- .

Further evidence comes from comparisons with the isostructural MOFs with different counteranions (**LVMOF-1-X** with $X^- = PF_6^-, ClO_4^-, Br^-$ or I^- , obtained by anion exchange. Detailed anion-exchange studies will be presented later). We found that **LVMOF-1-Br** is similar to **LVMOF-1-Cl** in hydro-, photo-, and piezochromism, while the PF_6^- , ClO_4^- , and I^- counterparts do not show any of these chromogenic properties. *The decisive impacts of anions on ET definitely confirm that the effective electron donor is an appropriate anion (Cl^- or Br^-) but not any groups from the framework or guest molecules.* The impacts of anions can be related to their vertical detachment energies (VDEs) or the electron affinities (EAs) of the corresponding neutral radical species. PF_6^- and ClO_4^- are among the so-called superhalogens because their VDEs (7.35 and 5.44 eV, respectively) well exceed the EA of chlorine (3.61 eV).^[23] The high VDEs mean poor electron-donor ability and justify the negative chromogenic response of **LVMOF-1- PF_6 / ClO_4** . By contrast, the lower EAs of Cl^- and Br^- (3.36 eV)^[24] dictate appropriate electron donor strength for ET to viologen. The negative impact of I^- , which has a still lower EA (3.06 eV),^[24] will be explained later.

To further verify that the electron donor is an appropriate anion not the MOF itself, we extended the study to more anions. It proved that the **LVMOF-1-X** MOFs with $X = NO_2^-$ and SO_3^{2-} behave like those with $X = Cl^-$ and Br^- , displaying obvious reversible color changes after dehydration, compression, or Xe-light photoirradiation in organic solvents. On the other hand, **LVMOF-1- MnO_4** does not show the color response. The results are consistent with the electron-donating nature of NO_2^- and SO_3^{2-} and the oxidative nature of MnO_4^- . For **LVMOF-1- MnO_4** , the UV-vis spectra show no changes after compression or dehydration (**Figure S6**, Supporting Information), precluding the possibility that the color change is obscured by the dark violet color of MnO_4^- .

The impacts of water on the ET chromogenic behaviors of **LVMOF-1** merit further discussion. The impacts are reflected in several aspects: i) the pristine MOF, which contains guest water, is nonphotochromic, but evacuating the MOF induces ET and the evacuated MOF becomes photochromic; ii) the MOF is photochromic in organic solvents but not in water; iii) the radical-containing states, whether generated by dehydration or photoirradiation, readily undergoes back ET on exposure to water. All of these observations suggest that *water molecules impede forward ET from chloride to viologen and promote back ET*. The impacts can be justified as follows. The highly polar water molecules interact with and stabilize V^{2+} and Cl^- by electrostatic forces and hydrogen bonds. The interactions reduce the acceptor/donor strength to the disadvantage of ET. Meanwhile, the high-polarity environments set by these interactions are disliked by electron-rich, less positive V^{+} and electron-deficient, neutral Cl^{\cdot} , so water destabilizes the radicals in favor of back ET. The effects of water are similar to those we have recently found for the pseudopolymorphs of an organic viologen molecule.^[19b]

For solvent-assisted photochromism, an important issue is whether the solvent molecule serves as electron donor. Control experiments with different solvents were performed to clarify the issue. First, photochromism of **LVMOF-1-Cl** was tested in various solvents with different electron-donor strength (measured by the IP values). We found that photochromism occurs not only in aforementioned solvents, which have lower IPs than water, but also in those with similar or higher IPs (acetonitrile, 12.20 eV; malononitrile, 12.80 eV). The IP independence implies that the solvents are not the necessary electron donors

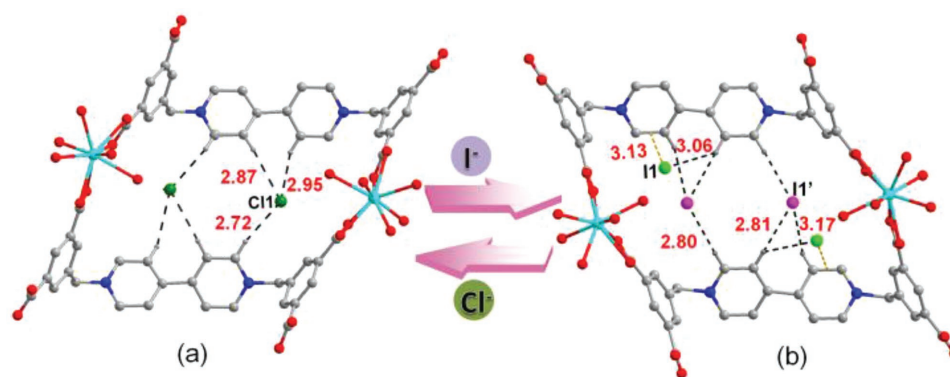


Figure 4. The anion-viologen interactions in a) **LVMOF-1-Cl** and b) **LVMOF-1-I**. The green and purple balls in (b) represent the disordered iodide ions at crystallographically independent positions.

for solvent-assisted photochromism. Second, **LVMOF-1-X**'s with $X^- = \text{PF}_6^-$, ClO_4^- , and I^- do not show photochromism in any of the solvents tested. This confirms that even the solvent with lower IP than water does not serve as electron donors. Having excluded the solvents from electron donors, we can safely say that solvent-assisted photochromism of **LVMOF-1** is because guest exchange facilitates $\text{V}^{2+} \leftarrow \text{Cl}^-$ ET: water molecules that impede ET are replaced by other solvent molecules, which have weaker or no polarity and hydrogen-bonding ability.

The combination of viologen and Eu(III) in one MOF opens the possibility of switching or modulating the Eu(III)-based luminescence through the diverse chemical or physical tools that induce viologen-based ET response. **LVMOF-1** shows excitation and emission spectra characteristic of Eu(III) f-f transitions, with ${}^7\text{F}_0 \rightarrow {}^5\text{L}_6$ (394 nm) and ${}^5\text{D}_0 \rightarrow {}^7\text{F}_2$ (614 nm), respectively, as the most intense.^[15] All of the stimuli that induce the MOF to undergo chromogenic response (water evacuation, photoirradiation after evacuation and in organic solvents, and pressure) can cause significant quenching of the Eu(III) luminescence (Figure 2e). Since there is a good overlap between the Eu(III) emission and the broad radical absorption in the 500–800 nm region, the quenching mechanism should be Förster resonance EnT (FRET) from excited Eu(III) to radicals (Figure S7, Supporting Information).^[25] The luminescence is recovered when the pristine yellow state is recovered at ambient pressure (in the case of piezochromism) or in moist air (other cases). Notably, the solvent-assisted photoresponse is very fast, the quenching efficiency reaching 80% after only 1 s irradiation (Figure S8, Supporting Information).

To gain more insight into the effects of pressure on luminescence, in situ high-pressure luminescence spectra were recorded using the DAC technique. As shown in Figure 3b, the emission intensity gradually decreases upon compression, agreeing with the incremental formation of radicals. The variation of the intensity with pressure follows an exponential decay function. The intensity is recovered by 52% after complete decompression (Figure S9, Supporting Information). The incomplete emission recovery is consistent with the incompletely disappeared radical absorption (vide supra) after complete removal of pressure. Another trend is the redshift of the emission peaks with increasing pressure. The shift of the main component (at about 610 nm) of the ${}^5\text{D}_0 \rightarrow {}^7\text{F}_2$ transition

(Figure 3c) is quasi-linear with a shift rate of 0.41 nm GPa^{-1} , falling within the range ($0.1\text{--}1.2 \text{ nm GPa}^{-1}$) reported for Eu(III) doped in some inorganic host materials.^[26] The peaks shift back to the original wavelengths after decompression, suggesting the shift is irrelevant to the presence of radicals. Instead, the redshift can be due to enhancement of the nephelauxetic effect under pressure:^[26,27] Pressure strengthens the Eu–O bonds and increases the covalence, which expands the electron cloud around the metal nucleus, mitigates the interelectronic repulsion, and thereby reduces the energy gaps between ${}^5\text{D}_0$ and ${}^7\text{F}_j$. This is the first report of pressure modulation of luminescence associated with PzET. The material has potential applications in high-pressure sensors with multiple readout signals (absorbance, emission intensity, and wavelength).

There have been a few Eu(III) MOFs showing photochromism (Table S2, Supporting Information),^[19c,25,28] all involving PET to bipyridinium species except for a bipyridinium-free MOF.^[28a] Only recently a hydrochromic Eu(III) MOF was reported,^[19c] which is also due to reversible ET to bipyridinium. No piezochromic Eu(III) MOF has been reported prior to **LVMOF-1**. The chromic bipyridinium moieties in above Eu(III) MOFs all allow for photoluminescence modulation through the different stimuli. In addition, among these chromic Eu(III) MOFs, **LVMOF-1** is the only one showing permanent open pores, which makes it possible to use the solvent molecules and anions as the handles to control the responsive properties.

2.2. Responsive Properties Associated with Anion Exchange

The stable cationic host of **LVMOF-1-Cl** allows reversible anion exchange, which can be performed by simply stirring the MOF in aqueous solutions of the target anions. The exchange with multivalent anions such as PF_6^- and ClO_4^- is evinced by the strong IR absorption characteristic of the anions (Figure S10, Supporting Information). Energy dispersive X-ray spectra and elemental maps confirm the disappearance of Cl^- and the uniform distribution of anions (Figure S11, Supporting Information). PXRD confirms the structural integrity of the framework after exchange (Figure S12, Supporting Information). The anion exchange is reversible.

Interestingly, ion exchange with I^- causes immediate color change to orange (Figure 5a), in high contrast to the pale

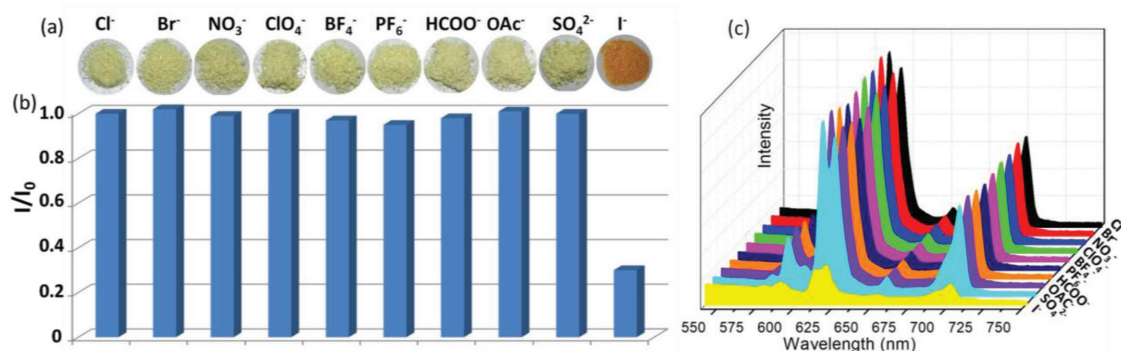


Figure 5. a) The colors of the solids obtained after anion exchange with different anions (as potassium salts, 1.0 M aqueous solutions). b) The relative intensity of the ${}^5\text{D}_0 \rightarrow {}^7\text{F}_2$ emission of the aqueous **LVMOF-1-Cl** suspension in response to different anions (1.0×10^{-3} M, excited at 394 nm). c) Photoluminescent spectra of the aqueous **LVMOF-1-Cl** suspension in response to different anions (1.0×10^{-3} M, excited at 394 nm).

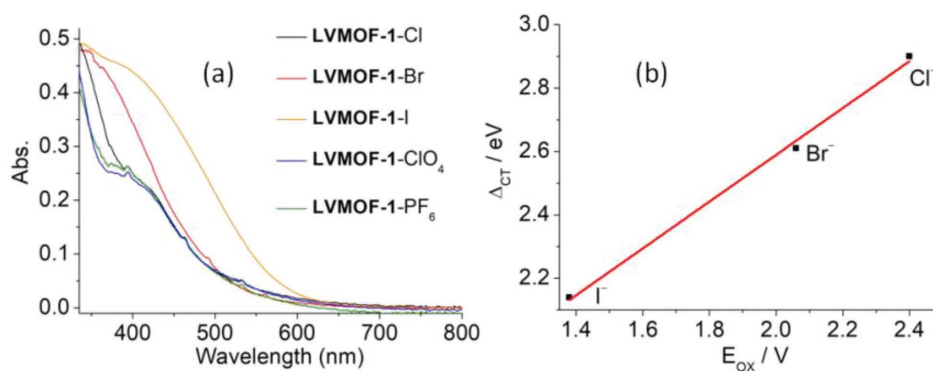


Figure 6. a) UV-vis spectra of LVMOF-1 with different anions. b) The Mulliken dependence: linear correlations of the CT transition energy (Δ_{CT}) to the oxidation potential (E_{ox} (X^-/X)) of the halides in water. Δ_{CT} was estimated from the CT band in the solid-state UV-vis spectrum.^[31]

yellow color for other anions (Cl^- , Br^- , NO_3^- , ClO_4^- , BF_4^- , PF_6^- , $HCOO^-$, CH_3COO^- , and SO_4^{2-}). The color and the significantly increased visible-light absorption of LVMOF-1-I (Figure 6a) are diagnostic of strong ground-state CT complexation between viologen and I^- . Compared with the MOFs with superhalogen anions such as PF_6^- and ClO_4^- , LVMOF-1-Cl and LVMOF-1-Br also show additional absorption below and around 400 nm, respectively. The absorption is indicative of weak CT complexes, which do not cause detectable difference in color. The spectra confirm the ability of the anions to form CT complexes with viologen decreases in the order $I^- > Br^- > Cl^- \gg ClO_4^-/PF_6^-$, consistent with the increase of VDEs or IPs (vide supra). The CT character of the absorption of the I^- , Br^- , and Cl^- MOFs is unequivocally established by Mulliken dependence,^[29] i.e., the CT transition energy (Δ_{CT}) estimated from the absorption is linearly correlated to oxidation potentials of the halides (Figure 6b).^[30,31]

To get structural evidences for CT interactions, single crystals of LVMOF-1-I have been prepared by single-crystal-to-single-crystal anion exchange between LVMOF-1-Cl and aqueous KI. X-ray crystallographic studies revealed that there are $H_V \cdots I$ (2.80–3.17 Å) and $I^- \cdots \pi$, interactions (I^- is hung above a pyridinium C–C edge with $I \cdots C = 3.13$ Å) (Figure 4). The anion $\cdots \pi$ interaction is absent in LVMOF-1-Cl and the $H_V \cdots I$ distances are similar to $H_V \cdots Cl$ (2.72–2.95 Å) despite the larger size of I^- . These data confirm stronger CT interactions in LVMOF-1-I.

Quite interestingly, the CT complexation has strong influence on ET activity. In the preceding section we have mentioned that anion exchange with I^- suppresses ET-based hydro-, photo-, and piezochromism. The reason can be partially because the fractional charge (δ) transferred in the CT complex ($V^{(2-\delta)+} - I^{(1-\delta)-}$) compensates the electron-donor/acceptor strength in disfavor of ET. In other words, CT interactions provide additional stabilization for the nonradical states of the donor and acceptor. In case of photoirradiation, photoexcitation of the CT complex may cause PET, but the excited PET state can decay through ultrafast back ET, which is so fast that no steady radical species can be detected. The PET and ultrafast back ET in the solid state could be similar to those in the solutions of viologen-iodide ion-pair CT complexes, which have been established by transient absorption spectroscopy.^[32] The ultrafast back ET

can be justified by considering the Marcus inverted region, wherein ET becomes faster as the driving force decreases.^[32a,33] Compared with other halides, the small oxidation potential (or IP) of I^- dictates a small driving force and thereby an ultrafast rate for the back ET.^[32] Alternatively, the ultrafast dynamics can be understood by considering that the strong CT interactions between donor and acceptor provide very efficient pathways for back ET.

The iodide-viologen CT complexation also causes a strong effect on photoluminescence properties, besides selective ionochromism and ET suppression. Iodide can efficiently switch off the Eu(III) luminescence (Figures S13 and S14, Supporting Information), while other anions have no significant effects (Figure 5b,c). Comparing the absorption and emission spectra of LVMOF-1-I reveals some overlap between the CT absorption and the ${}^5D_0 \rightarrow {}^7F_{0/1}$ emission, so the quenching effect can be attributed to FRET from Eu(III) to the CT complex. Electrochemical studies were performed to gain insight into the FRET process. As shown in Figure 7a, the cyclic voltammograms of LVMOF-1-X show two pairs of anodic and cathodic peaks attributable to V^{2+}/V^{+} and V^{+}/V^0 .^[3a] According to E_{LUMO} (LUMO = lowest unoccupied molecular orbital) estimated from the first reduction potential and Δ_{CT} estimated from the CT absorption in the solid-state UV-vis spectra,^[31,34] the Jablonski diagram for EnT in LVMOF-1-X is drawn in Figure 7b. The highest occupied molecular orbital for LVMOF-1-I is significantly higher than those for the Br^- and Cl^- counterparts, reflecting the stronger donor ability of I^- . The CT transition energy (2.14 eV) for LVMOF-1-I well matches the ${}^5D_0 \rightarrow {}^7F_0$ transition energy ($\approx 17\,200\text{ cm}^{-1}$, or 2.14 eV) of Eu(III), so EnT can occur through electronic dipolar resonance, giving rise to luminescence quenching. The CT gaps for LVMOF-1-Br/Cl are too large for FRET, so the Eu(III) luminescence is not quenched.

2.3. Applications

The versatile responsive properties of LVMOF-1 have important implications for applications, such as multimode switches for which visible-light absorption and luminescence can be turned on/off with various stimuli. The on/off switching of and luminescence (as outputs) can be used to mimic Boolean

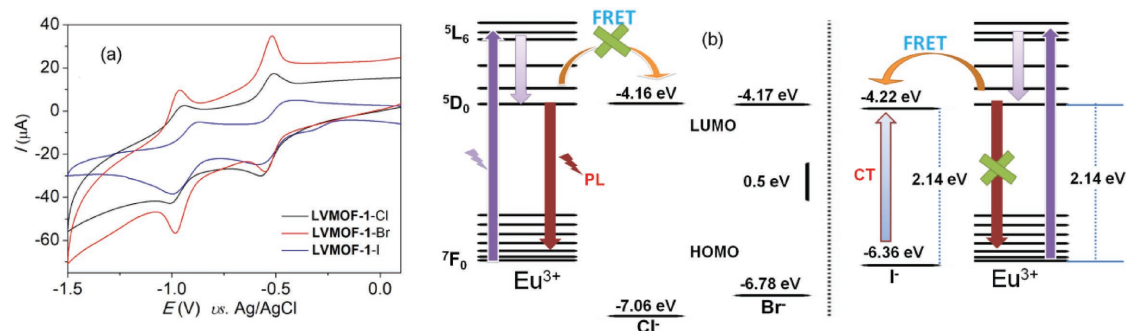


Figure 7. a) Cyclic voltammograms for LVMOF-1-X. b) The Jablonski diagram for EnT in LVMOF-1-X.

logic gates.^[35] Let us consider Xe light and an organic solvent (ethanol, for example) as two inputs operating on LVMOF-1-Cl. On the basis of solvent-assisted photochromism, the absorption and luminescence outputs are turned on and off, respectively, only if the two inputs coexist (Figure 8). The logic gates correspond to the AND and NAND logic gates, respectively. The logic gates can reset by treating the material with water. Moreover, including another organic solvent in the system can lead to two integrated logic gates (enabled OR and NOR,^[36] Figure S15, Supporting Information), where the logic functions (OR and NOR) of two inputs (the two solvents) are evoked only in the presence of the third input (light).

Selective and sensitive detection of iodine has attracted much attention for its essential importance to life, for the concerns about its discharge to environments, and also for the growing need in radionuclide monitoring in nuclear industry.^[37] The selective ionochromic and luminescence response of LVMOF-1-Cl inspires us to investigate its performance as a sensor for detecting I^- in water.

For qualitative detection, test paper strips were prepared by dip-coating filter paper in aqueous suspension of LVMOF-1-Cl. The test paper shows immediate color response to aqueous I^- , with good selectivity against various common anions (Figure 9a). Moreover, the used test paper can be recovered and reused after immersion in KCl solution for a few hours. The test paper demonstrates a facile, portable, selective, rapid, and recyclable method for on-site detection of I^- .

Luminescence titration experiments were performed to demonstrate quantitative detection of I^- using LVMOF-1-Cl. The results (Figure 9b) show that the emission intensity of the MOF dispersed in water decreases with incremental addition of I^- . At $[\text{I}^-] = 1 \times 10^{-3} \text{ M}$, the quenching efficiency is 70%, which is defined by $(I_0 - I)/I_0 \times 100\%$ (I_0 and I are the intensity of the $5D_0 \rightarrow 7F_2$ emission in the absence and presence of the analyte). In the low concentration range, the intensity is correlated to $[\text{I}^-]$ according to the linear Stern–Volmer equation $I_0/I = K_{sv}[\text{I}^-] + 1$ with $K_{sv} = 4.2 \times 10^3 \text{ M}^{-1}$. The detection limit (DL) is $1.8 \times 10^{-6} \text{ M}$ (0.20 ppm) according to $3\sigma/K_{sv}$, where σ is the standard deviations (σ) for I_0/I

at low concentrations. The DL is good in comparison with other I^- ion fluorescence sensors (Table S3, Supporting Information). We also determined the performance of LVMOF-1-ClO₄ and LVMOF-1-PF₆ for detection of I^- (Figures S16 and S17, Supporting Information). The K_{sv} values and detection limits are very similar to those for LVMOF-1-Cl. Because the detection of I^- using the different MOFs is based on the same quenching mechanism (EnT from $\text{Eu}(\text{III})$ to the I^- -viologen CT complex), it is reasonable that the anion with no significant CT ability imposes little influence on the detection performance.

The response rate is a very important factor for real-time detection. According to time-dependent luminescence measurements, the quenching efficiency of the 614 nm emission becomes constant in 5 s after I^- addition (Figure S18, Supporting Information). Such a short response time is rare for chemical sensing.^[37,38] It suggests a very fast kinetics for anion exchange with I^- , which can be related to the open channels provided by the structure and the strong driving force arising from the receptor-analyte CT affinity. In addition, the stability and anion-exchangeability of the ionic MOF facilitates regeneration and reuse. After sensing use, the material can be

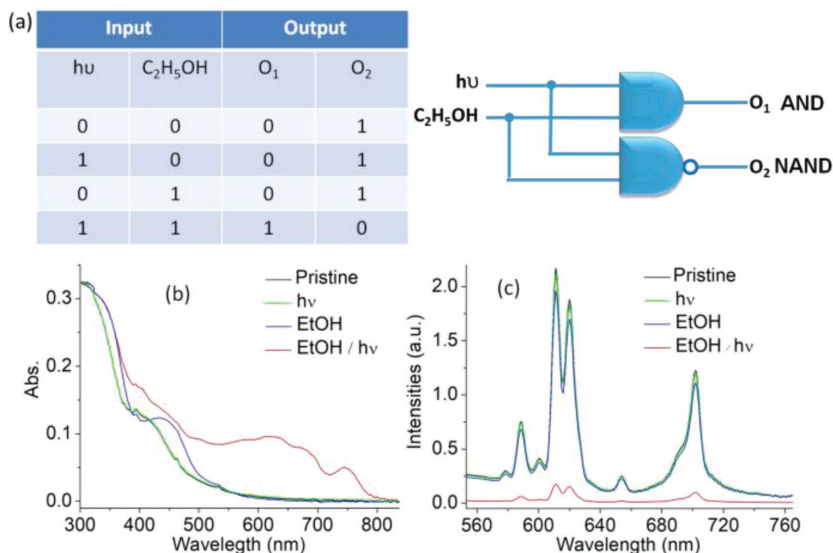


Figure 8. a) Truth tables and logic circuit for the AND and NAND gates. O_1 and O_2 represent the absorbance and luminescence outputs, respectively. b) UV-vis and c) luminescence spectra for the LVMOF-1-Cl based gates with different input combinations.

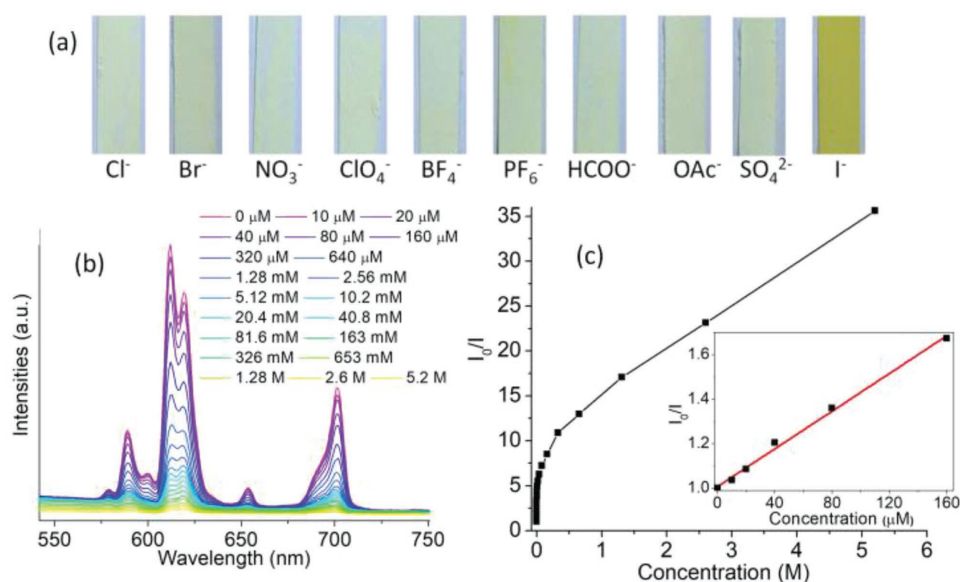


Figure 9. a) Photographs of the LVMOF-1-Cl coated test papers after treatment with different anions in water (1.0×10^{-3} M). b) Emission spectra ($\lambda_{\text{ex}} = 394$ nm) of the LVMOF-1-Cl aqueous dispersion (0.75 mg mL^{-1} , pH = 7) with the incremental addition of KI aqueous solution at room temperature (the KI concentrations are labeled). c) Stern–Volmer curve acquired from the $^5\text{D}_0 \rightarrow ^7\text{F}_2$ transition. Inset: Linear fit (red line, $R^2 = 0.995$) in the low concentration region.

regenerated simply by centrifugation and washing with KCl solutions. After five cycles, the luminescence response to I⁻ shows no obvious change (Figure 10a). Finally, the anti-jamming capability of the MOF was tested. As shown in Figure 10b, the luminescence response to I⁻ is hardly interfered by Cl⁻ and Br⁻.

3. Conclusion

In summary, all of the components (the metal center and viologen ligand constituting the cationic framework, the guest counteranion and solvent occupying the open channel) in LVMOF-1 are mobilized to directly participate in or indirectly influence the ET, CT and EnT processes, resulting in remarkably versatile responsive properties. Stimuli-induced ET between anion (Cl⁻/Br⁻) and viologen generates radicals and leads to reversible piezochromism, hydrochromism, and photochromism. Strong ground-state CT complexation between iodide and viologen leads to selective ionochromism. Resonance EnT from Eu(III) to the CT complex or the ET-generated radical leads to luminescence quenching. The guest water and anion serve as flexible handles to control the responsive properties. The water molecules impede forward ET and promote back ET, so water release/reuptake or solvent exchange can turn on/off photochromism. Anion exchange of LVMOF-1-Cl⁻/Br⁻ with poor electron donors such as PF₆⁻ and ClO₄⁻ precludes ET and thus turns off the response to pressure, light, and water release/reuptake. The formation of stable ground-state complexes between I⁻ and viologen also suppresses the ET-based response. It is remarkable to observe so versatile and flexible responsive properties in one material. The properties enable us to demonstrate the potential use in chemical logic gates and sensors. Particularly, the colorimetric test paper deposited with the MOF provides a facile and portable method for on-site

qualitative detection of I⁻ in water, while the luminescence response allows convenient quantitative determination at micro-molar concentration. The methods feature fast response, good

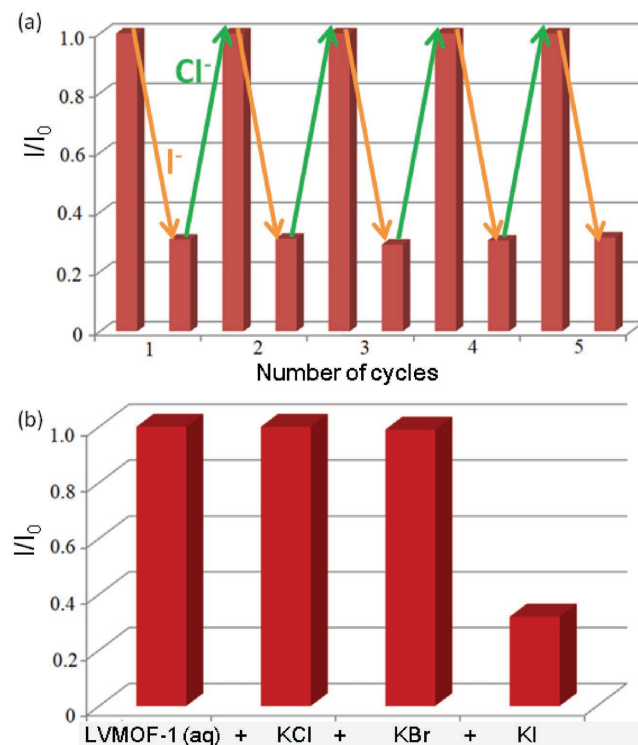


Figure 10. a) Five cycle tests of LVMOF-1-Cl for sensing I⁻ ions. The concentrations of Cl⁻ and I⁻ ions are 1 M and 1×10^{-3} M, respectively. b) Relative intensity for the $^5\text{D}_0 \rightarrow ^7\text{F}_2$ emission of the LVMOF-1-Cl aqueous dispersion as KCl, KBr and KI were successively added. The concentration of each analyte is 1×10^{-3} M.

antijamming performance, and excellent recyclability. The work illustrates that viologen-based ionic MOFs are powerful platforms to manipulate ET, CT, and EnT in solid state. Extended work along the line will not only lead to new responsive materials but also add much to the understanding of these basic processes.

4. Experimental Section

All the reagents and solvents employed were commercially available and used without further purification. *Perchlorate has the risk of explosion and should be handled carefully with small amounts.* LVMOF-1 was synthesized by the literature procedures reported by us.^[15]

In Situ High-Pressure Spectroscopy: The *in situ* UV–vis absorption measurements under high pressure were performed on an Ocean Optics QE65000 scientific-grade spectrometer with a DAC (300 mm culets) containing a single crystal of LVMOF-1. A ruby sphere was loaded to determine pressure by using the ruby fluorescence, and silicone oil was used as a pressure-transmitting medium. The *in situ* luminescence spectra were obtained in a DAC (500 mm culets) using a Renishaw 1000 spectrometer with a 532 nm excitation laser.

Anion Exchange: LVMOF-1 (30 mg) was immersed in an aqueous solution (3 mL, 0.1 M) of KX (X = Br⁻, I⁻, ClO₄⁻, PF₆⁻) for one day. The solid is collected by filtration, washed with water, and then dried in air. The anion exchange proceeded in the single-crystal to single-crystal manner if single crystals of LVMOF-1 were used for exchange with I⁻. Elemental analysis calc. for [Eu₂(OH)₂(H₂O)₂L]₁₂·4H₂O (LVMOF-1-I, C₂₈H₃₂N₂O₁₆Eu₂): C, 27.78; H, 2.66; N, 2.31; Found: C, 27.51; H, 3.01; N, 2.65%. IR (KBr pellet, cm⁻¹): 3359br, 3043s, 1637m, 1616s, 1556 versus, 1454 versus, 1392 versus, 1168m, 775s, 725s.

Single Crystal X-Ray Crystallography: The details for X-ray analysis of LVMOF-1-I are provided in the Supporting Information. CCDC 1579918 contains the supplementary crystallographic data for this paper. These data can be obtained free of charge from The Cambridge Crystallographic Data Centre via www.ccdc.cam.ac.uk/data_request/cif.

Supporting Information

Supporting Information is available from the Wiley Online Library or from the author.

Acknowledgements

The authors acknowledge the financial support from the National Natural Science Foundation of China (NSFC Grant Nos. 21471057, 21773070, and 21805090), and China Postdoctoral Science Foundation (Grant No. 2018M632060). The authors thank X.-L. Bao (Instrumental Analysis Center of Shanghai Jiao Tong University) for help with X-ray crystallographic analysis.

Conflict of Interest

The authors declare no conflict of interest.

Keywords

charge transfer, electron transfer, luminescence switches, metal–organic frameworks, piezochromism

Received: August 26, 2018

Revised: October 15, 2018

Published online: January 9, 2019

- [1] a) S.-C. Wei, M. Pan, K. Li, S. Wang, J. Zhang, C.-Y. Su, *Adv. Mater.* **2014**, *26*, 2072; b) C. Qin, Y. Feng, H. An, J. Han, C. Cao, W. Feng, *ACS Appl. Mater. Interfaces* **2017**, *9*, 4066; c) F. Pilate, R. Mincheva, J. De Winter, P. Gerbaux, L. Wu, R. Todd, J.-M. Raquez, P. Dubois, *Chem. Mater.* **2014**, *26*, 5860; d) R. Xu, Y. Wang, X. Duan, K. Lu, D. Micheroni, A. Hu, W. Lin, *J. Am. Chem. Soc.* **2016**, *138*, 2158; e) W. Ke, W. Yin, Z. Zha, J. F. Mukerabigwi, W. Chen, Y. Wang, C. He, Z. Ge, *Biomaterials* **2018**, *154*, 261.
- [2] a) H. Furukawa, K. E. Cordova, M. O'Keeffe, O. M. Yaghi, *Science* **2013**, *341*, 1230444; b) L. E. Kreno, K. Leong, O. K. Farha, M. Allendorf, R. P. Van Duyne, J. T. Hupp, *Chem. Rev.* **2012**, *112*, 1105; c) B. Li, H. M. Wen, Y. Cui, W. Zhou, G. Qian, B. Chen, *Adv. Mater.* **2016**, *28*, 8819; d) R.-W. Huang, Y.-S. Wei, X.-Y. Dong, X.-H. Wu, C.-X. Du, S.-Q. Zang, T. C. W. Mak, *Nat. Chem.* **2017**, *9*, 689; e) L. Chen, J. W. Ye, H. P. Wang, M. Pan, S. Y. Yin, Z. W. Wei, L. Y. Zhang, K. Wu, Y. N. Fan, C. Y. Su, *Nat. Commun.* **2017**, *8*, 15985.
- [3] a) P. M. S. Monk, *The Viologens. Physicochemical Properties, Synthesis and Applications of the Salts of 4,4'-Bipyridine*, John Wiley & Sons Ltd., Chichester **1998**; b) G. Xu, G.-C. Guo, M.-S. Wang, Z.-J. Zhang, W.-T. Chen, J.-S. Huang, *Angew. Chem., Int. Ed.* **2007**, *46*, 3249; c) A. T. Buck, J. T. Paletta, S. A. Khinduranga, C. L. Beck, A. H. Winter, *J. Am. Chem. Soc.* **2013**, *135*, 10594; d) T. Fiala, L. Ludvikova, D. Heger, J. Svec, T. Slanina, L. U. Vetrakova, M. Babiak, M. Necas, P. Kulhanek, P. Klan, V. Sindelar, *J. Am. Chem. Soc.* **2017**, *139*, 2597; e) X. Gong, R. M. Young, K. J. Hartlieb, C. Miller, Y. Wu, H. Xiao, P. Li, N. Hafezi, J. Zhou, L. Ma, T. Cheng, W. A. Goddard, O. K. Farha, J. T. Hupp, M. R. Wasielewski, J. F. Stoddart, *J. Am. Chem. Soc.* **2017**, *139*, 4107.
- [4] a) H. C. Moon, T. P. Lodge, C. D. Frisbie, *Chem. Mater.* **2015**, *27*, 1420; b) J. Wang, S. L. Li, X. M. Zhang, *ACS Appl. Mater. Interfaces* **2016**, *8*, 24862.
- [5] Q.-X. Yao, L. Pan, X.-H. Jin, J. Li, Z.-F. Ju, J. Zhang, *Chem. - Eur. J.* **2009**, *15*, 11890.
- [6] a) Y. Wang, M. Frasconi, J. F. Stoddart, *ACS Cent. Sci.* **2017**, *3*, 927; b) L. Striepe, T. Baumgartner, *Chem. - Eur. J.* **2017**, *23*, 16924.
- [7] a) K. Kawano, K. Yamauchi, K. Sakai, *Chem. Commun.* **2014**, *50*, 9872; b) A. J. Bard, M. A. Fox, *Acc. Chem. Res.* **1995**, *28*, 141.
- [8] J.-K. Sun, J. Zhang, *Dalton Trans.* **2015**, *44*, 19041.
- [9] H.-Y. Li, Y.-L. Wei, X.-Y. Dong, S.-Q. Zang, T. C. W. Mak, *Chem. Mater.* **2015**, *27*, 1327.
- [10] a) T. Gong, X. Yang, Q. Sui, Y. Qi, F.-G. Xi, E.-Q. Gao, *Inorg. Chem.* **2016**, *55*, 96; b) T. Gong, P. Li, Q. Sui, L.-J. Zhou, N.-N. Yang, E.-Q. Gao, *Inorg. Chem.* **2018**, *57*, 6791.
- [11] P. X. Li, M. S. Wang, M. J. Zhang, C. S. Lin, L. Z. Cai, S. P. Guo, G. C. Guo, *Angew. Chem., Int. Ed.* **2014**, *53*, 11529.
- [12] C. Sun, M. S. Wang, P. X. Li, G. C. Guo, *Angew. Chem., Int. Ed.* **2017**, *56*, 554.
- [13] J.-K. Sun, X.-D. Yang, G.-Y. Yang, J. Zhang, *Coord. Chem. Rev.* **2017**, *378*, 533.
- [14] M. Higuchi, K. Nakamura, S. Horike, Y. Hijikata, N. Yanai, T. Fukushima, J. Kim, K. Kato, M. Takata, D. Watanabe, *Angew. Chem.* **2012**, *124*, 8494.
- [15] T. Gong, P. Li, Q. Sui, J. Chen, J. Xu, E.-Q. Gao, *J. Mater. Chem. A* **2018**, *6*, 9236.
- [16] a) B. Odell, M. V. Reddington, A. M. Z. Slawin, N. Spencer, J. F. Stoddart, D. J. Williams, *Angew. Chem., Int. Ed. Engl.* **1988**, *27*, 1547; b) P. R. Ashton, B. Odell, M. V. Reddington, A. M. Z. Slawin, J. F. Stoddart, D. J. Williams, *Angew. Chem., Int. Ed. Engl.* **1988**, *27*, 1550; c) M. Frasconi, I. R. Fernando, Y. Wu, Z. Liu, W.-G. Liu, S. M. Dyar, G. Barin, M. R. Wasielewski, W. A. Goddard, J. F. Stoddart, *J. Am. Chem. Soc.* **2015**, *137*, 11057.
- [17] R.-G. Lin, G. Xu, M.-S. Wang, G. Lu, P.-X. Li, G.-C. Guo, *Inorg. Chem.* **2013**, *52*, 1199.

- [18] P. Bamfield, M. G. Hutchings, *Chromic Phenomena: Technological Applications of Colour Chemistry*, 2nd ed., RSC, Cambridge **2010**.
- [19] a) Q. Sui, X.-T. Ren, Y.-X. Dai, K. Wang, W.-T. Li, T. Gong, J.-J. Fang, B. Zou, E.-Q. Gao, L. Wang, *Chem. Sci.* **2017**, *8*, 2758; b) Q. Sui, N.-N. Yang, T. Gong, P. Li, Y. Yuan, E.-Q. Gao, L. Wang, *J. Phys. Chem. Lett.* **2017**, *8*, 5450; c) C. Zhang, L. Sun, Y. Yan, H. Shi, B. Wang, Z. Liang, J. Li, *J. Mater. Chem. C* **2017**, *5*, 8999; d) T. Gong, X. Yang, J.-J. Fang, Q. Sui, F.-G. Xi, E.-Q. Gao, *ACS Appl. Mater. Interfaces* **2017**, *9*, 5503.
- [20] Q. Sui, Y. Yuan, N.-N. Yang, X. Li, T. Gong, E.-Q. Gao, L. Wang, *J. Mater. Chem. C* **2017**, *5*, 12400.
- [21] Z.-W. Chen, G. Lu, P.-X. Li, R.-G. Lin, L.-Z. Cai, M.-S. Wang, G.-C. Guo, *Cryst. Growth Des.* **2014**, *14*, 2527.
- [22] a) J. Peon, X. Tan, J. D. Hoerner, C. Xia, Y. F. Luk, B. Kohler, *J. Phys. Chem. A* **2001**, *105*, 5768; b) J. D. Henrich, S. Suchyta, B. Kohler, *J. Phys. Chem. B* **2015**, *119*, 2737.
- [23] a) G. L. Gutsev, *J. Chem. Phys.* **1993**, *98*, 444; b) A. K. Srivastava, A. Kumar, N. Misra, *New J. Chem.* **2017**, *41*, 5445.
- [24] J. A. Dean, *Lange's Handbook of Chemistry*, 13th ed., McGraw-Hill Book Company, New York **1985**.
- [25] H. Y. Li, H. Xu, S. Q. Zang, T. C. Mak, *Chem. Commun.* **2015**, *52*, 525.
- [26] J. Zhang, H. Cui, P. Zhu, C. Ma, X. Wu, H. Zhu, Y. Ma, Q. Cui, *J. Appl. Phys.* **2014**, *115*, 023502.
- [27] D. Machon, V. P. Dmitriev, V. V. Sinitsyn, G. Lucazeau, *Phys. Rev. B* **2004**, *70*, 094117.
- [28] a) Y. N. Gong, X. W. Wei, J. H. Deng, D. C. Zhong, C. Y. Pan, *Dalton Trans.* **2017**, *46*, 15656; b) J. K. Sun, L. X. Cai, Y. J. Chen, Z. H. Li, J. Zhang, *Chem. Commun.* **2011**, *47*, 6870; c) H. Chen, G. Zheng, M. Li, Y. Wang, Y. Song, C. Han, J. Dai, Z. Fu, *Chem. Commun.* **2014**, *50*, 13544; d) X. Du, H. Li, H. Liu, G. Li, L. Li, S. Zang, *Chin. J. Appl. Chem.* **2017**, *34*, 1024.
- [29] a) S. Guha, F. S. Goodson, L. J. Corson, S. Saha, *J. Am. Chem. Soc.* **2012**, *134*, 13679; b) R. S. Mulliken, *J. Am. Chem. Soc.* **1952**, *74*, 811.
- [30] P. Wardman, *J. Phys. Chem. Ref. Data* **1989**, *18*, 1637.
- [31] P. Sippel, D. Denysenko, A. Loidl, P. Lunkenheimer, G. Sastre, D. Volkmer, *Adv. Funct. Mater.* **2014**, *24*, 3885.
- [32] a) F. Ito, T. Nagamura, *J. Photochem. Photobiol., C* **2007**, *8*, 174; b) W. Jarzęba, S. Pommeret, J.-C. Mialocq, *Chem. Phys. Lett.* **2001**, *333*, 419.
- [33] a) J.-L. Brédas, D. Beljonne, V. Coropceanu, J. Cornil, *Chem. Rev.* **2004**, *104*, 4971; b) C.-C. Chiu, C.-C. Hung, P.-Y. Cheng, *J. Phys. Chem. B* **2016**, *120*, 12390.
- [34] C. M. Cardona, W. Li, A. E. Kaifer, D. Stockdale, G. C. Bazan, *Adv. Mater.* **2011**, *23*, 2367.
- [35] A. P. de Silva, N. D. McClenaghan, *Chem. - Eur. J.* **2004**, *10*, 574.
- [36] A. Roque, F. Pina, S. Alves, R. Ballardini, M. Maestri, V. Balzani, *J. Mater. Chem.* **1999**, *9*, 2265.
- [37] P. F. Shi, H. C. Hu, Z. Y. Zhang, G. Xiong, B. Zhao, *Chem. Commun.* **2015**, *51*, 3985.
- [38] W. P. Lustig, S. Mukherjee, N. D. Rudd, A. V. Desai, J. Li, S. K. Ghosh, *Chem. Soc. Rev.* **2017**, *46*, 3242.